IN 35
077244

FINAL REPORT

NASA GRANT NAG 2-1062

FAR-INFRARED HETERODYNE SPECTROMETER FOR SOFIA

Period: April 1, 1996 through December 31, 1998

A. L. Betz, Principal Investigator

Center for Astrophysics & Space Astronomy,
University of Colorado, Boulder, CO 80309

ABSTRACT

This report summarizes work done under NASA Grant NAG2-1062 awarded to the University of Colorado. The project goal was to evaluate the scientific capabilities and technical requirements for a far-infrared heterodyne spectrometer suitable for the SOFIA Airborne Observatory, which is now being developed by NASA under contract to the Universities Space Research Association (USRA). The conclusions detailed below include our specific recommendations for astronomical observations, as well as our intended technical approach for reaching these scientific goals. These conclusions were presented to USRA in the form of a proposal to build this instrument. USRA subsequently awarded the Univerisity of Colorado a 3-year grant (USRA 8500-98-010) to develop the proposed Hot-Electron micro-Bolometer (HEB) mixer concept for high frequencies above 3 THz, as well as other semiconductor mixer technologies suitable for high sensitivity receivers in the 2-6 THz frequency band.

FINAL REPORT - NASA Grant NAG 2-1062

A Far-Infrared Heterodyne Spectrometer for SOFIA

A. L. Betz and R. T. Boreiko

Center for Astrophysics and Space Astronomy, University of Colorado, Boulder, CO 80309

1. Introduction

This final report for NASA Grant NAG 2-1062 "A Far-Infrared Heterodyne Spectrometer for SOFIA" describes work performed during the original 9-month grant period from 4-01-96 to 12-31-96, plus no-cost extension periods ending 12-31-98. The project was a design study to optimize the design of a far-infrared heterodyne spectrometer for the 50-300 μm spectral region that could eventually be used on the SOFIA Observatory. As part of the design study, we investigated two mixer technologies for far-infrared detection : quasioptical hot-electron microbolometers and Ga:Ge blocked-impurity band photomixers, as well as three possible local oscillator solutions not previously used successfully for infrared astronomy: cascaded multipliers, laser beat frequency synthesis, and laser sideband generation.

The final instrument design is reported here along with discussions of the comparative technologies that were examined. This discussion is preceded, however, by a summary of the particular science investigations in astronomy which motivate the effort. The main result from the project was a refined instrument proposal that was submitted to USRA, the prime contractor to NASA for the SOFIA project. USRA subsequently awarded us a detector development grant (USRA 8500-98-010) to extend the work on HEB mixers described here.

The spectrometer is ideally suited for observations of interstellar gas in regions of moderate and high excitation, especially the cores of interstellar clouds where UV- and shock-excitation are available. A sensitivity approaching the quantum noise limit and the high spectral resolution of a heterodyne receiver, combined with SOFIA's large aperture, will provide an observational facility unparalleled by any existing or planned space mission for far-infrared astronomical spectroscopy. The following report describes the science we want to do and how we intend to do it. The instrument is a dual band spectrometer with a sensitivity better than 10 hν per unit bandwidth. This far-infrared sensitivity compares favorably with the current state-of-the-art of 4 hν sensitivity for heterodyne spectrometers at submillimeter and mid-infrared wavelengths. Our SOFIA spectrometer will have a resolving power exceeding 10^6 and be able to observe 2 or more lines simultaneously with 3000 spectral channels of 0.3 km s^{-1} resolution. The new instrument is a second generation version of the heterodyne spectrometer we used successfully on the KAO for 11 years

(Boreiko & Betz 1995). The advantages (and disadvantages) of the new design are discussed in light of other observational capabilities planned for the wavelength region of interest: 50-200 μm. Items which may be called "new technology" are specifically identified, and the rewards and risks associated with their development are discussed.

Heterodyne spectroscopy is the most practical and sensitive method for achieving 1 km s^{-1} resolution at far-infrared wavelengths. This resolution is required to make full use of the information on dynamics available from the shapes and positions of spectral line profiles. The advantages and capabilities of the technique have been amply demonstrated with the first generation spectrometer flown aboard the KAO for over 10 years. The second generation instrument described here will not only take full advantage of the superior spatial resolution available from SOFIA, but also make efficient use of flight time by undertaking multiple simultaneous observations with near quantum-noise-limited sensitivity. Although the technical goals seem ambitious compared to current capabilities, recent breakthroughs in HEB mixer technology make the effort actually easier than it may at first appear.

The report is divided into 3 areas: selected scientific goals, final instrument design, and operational issues for the instrument onboard NASA's SOFIA Airborne Observatory. The work was done by the P.I. Albert Betz, Betz, the co-I Rita Boreiko, together with postdoc Philip Duggan and graduate student Yongxin Luo.

2. Scientific Program: Star Formation and Astrochemistry

Star formation and the physical processes underlying its initiation are a key research theme for the instrument. Information on this fundamental process can be gathered by observing far-infrared radiation emanating from the dense cores of molecular clouds - the so-called "stellar nurseries". These regions are typically 5-15" in size, and a telescope aperture of 2-3 m is needed for the diffraction limit field of view (FOV) to be comparable in angular size. Measurements of temperature, density, composition, and dynamics can all be made by observing spectral line radiation from atomic and molecular gas within these cores. Gas temperatures in star formation regions are typically in the range of 30-100 K. At such temperatures the peak of the blackbody curve falls at far-infrared wavelengths and line emission is strongest between 30-100 μm if the gas is in thermal equilibrium. Ideally, observations of line emission should be done with a spectral resolution adequate to identify the various cloud components by means of their differing Doppler shifts. In addition, measurements of the shapes of individual line profiles provide further discrimination between quiescent and shock-excited gas. All sorts of dynamical effects (outflows, infalls, shocks, jets, and rotation) can be measured by instruments with good spectral and spatial resolution. The required spectral resolution is governed by the widths of the narrowest features, which are about 1 km s^{-1}. A resolving power of 10^6 is consequently necessary, if it can be obtained without compromise in sensitivity.

Not all line emission is so narrow, of course. Shock excitation can produce line widths exceeding 100 km s^{-1} (FWZM), and so a wide observing bandwidth of 4 GHz (400 km s^{-1} at 3 THz) is also important. Fortunately the technology of the 1990's is up to the challenge, and it is now possible to do "radio astronomy" up to 6 THz (50 μm).

Because the core regions are so small, close to the diffraction limit of SOFIA in the far-infrared, extensive spatial mapping is not usually required, although for certain complex sources it would be desirable. Hence, in designing the instrument we stress spectral resolution over total spatial FOV. Other planned instruments with lower spectral resolution but with large array detectors are more appropriate for large scale mapping. Large scale mapping can also be done with smaller telescopes than SOFIA (if such were available). Nevertheless, we will design in a small array capability (6-8 elements) for our spectrometer to enable limited but perhaps adequate "imaging" of core regions. Arrays beyond this size become difficult for us to use from a data handling point of view. Remember each spatial element requires a multichannel "back-end" to analyze the line radiation. Radio telescopes currently use small 8-10 element arrays in the focal plane, and find the data rate manageable. We do not anticipate actually installing spatial arrays in the spectrometer until after the second year of flights with the multiband spectrometer.

Heterodyne spectroscopy offers the potential to achieve the Doppler-limited resolution we require together with the high sensitivity we also must have. Theoretically, a heterodyne receiver can achieve a sensitivity of η^{-1} photons per second per unit bandwidth: $P_{noise}/B = \nu/\eta$, where η is the effective quantum efficiency. This is the so-called quantum-noise-limit for receivers using coherent detection. The established technology of GaAs Schottky diode mixers at best achieves $\eta = 1\%$ at far-infrared wavelengths (Betz & Boreiko 1993), so there is considerable room for improvement. The factor of 10 increase in sensitivity with HEB mixers compared to Schottky diodes, plus the larger aperture of SOFIA compared to the KAO, will speed line detections in small sources (e.g., cloud cores and stellar sources) by a factor of 10^4. Entirely new problems can now be investigated on SOFIA that would never have been considered in the days of the KAO.

2.1. The Value of Resolution

We can simplistically classify all observations into two groups based on the ultimate signal-to-noise ratio of the measurement: (1) High signal-to-noise observations are those which are easily done but must be done repeatedly, for example mapping line emission or observing a large variety of sources in order to measure some global property of the emission. It has been our experience on the KAO that such observations are popular with GI teams, who need KAO observations to complement existing radio- or near-IR data. Examples would be observations of high-J CO, C II , and O I - all major cooling lines for warm molecular clouds. (2) Low signal-to-noise observations usually deal with the detection

of a weak line in a small number of sources, with the intent being species identification or an isotopic ratio measurement. In such observations, high resolution is essential for unambiguous line identification.

To illustrate the added insight one can get by re-examining previously detected line emission at higher spectral resolution, we present two examples from the KAO: high-J CO and OH rotational emission.

2.1.1. High-J CO Emission

The high-J transitions of CO between J=9-8 and J=36-35 lie in the far-infrared and selectively probe hotter and denser gas than that seen at millimeter wavelengths. For the sources W3, W51, M17, and DR21, we have observed the $J = 12 \rightarrow 11$, $J = 14 \rightarrow 13$, and $J = 16 \rightarrow 15$ transitions, and for W3, the $^{13}CO J = 14 \rightarrow 13$ line as well (Boreiko & Betz 1997). Figure 1 shows the ^{13}CO spectra obtained from W3 IRS5. It is immediately obvious that the CO lines are narrow with FWHM $\leq$ 10 km s^{-1}. This is the case for all 4 sources. Older Fabry-Perot observations of CO J=16→15 in W51 indicated a linewidth of $\sim$70 km s^{-1} FWHM (Jaffe, Harris, and Genzel 1987), which led to the conclusion that high-J CO emission in dense clouds was a product of high velocity shock excitation (Stutzki et al. 1988). The newer heterodyne observations show that the gas is more likely heated by UV radiation. The high-J CO lines are in fact even narrower than those seen in $^{12}CO J = 1 \rightarrow 0$ from the quiescent molecular cloud, or in the 158 μm fine-structure line of C^+ from the PDR (with similar beamsize). Obviously the dense parts of these clouds are compact with low velocity dispersions. They are nevertheless dynamically linked because of the identical V_{LSR} values for high and low-J CO and C II . Here we have a simple example that shows that high resolution is not merely a luxury, but a necessity, if proper interpretation of the data is to be obtained.

2.1.2. OH Rotational Emission

The emission from far infrared rotational lines of OH near IRc2 in M42 has generally been interpreted as coming from shock excited material. In this particular source the evidence for shock excitation of CO and H_2 is irrefutable. Whether this excitation is also responsible for the emission seen from OH, and whether it is responsible for the amount of OH seen, are questions worthy of further study. Hydrodynamic shock models (Draine, Roberge, and Dalgarno 1983) predict an OH abundance enhancement of about a factor of 25 in the postshock material relative to the cooler gas downstream.

The 119 μm and 163 μm lines of OH have previously been observed with a Fabry-Perot spectrometer at a resolution as fine as 24 km s^{-1}(Melnick et al. 1990). Comparisons
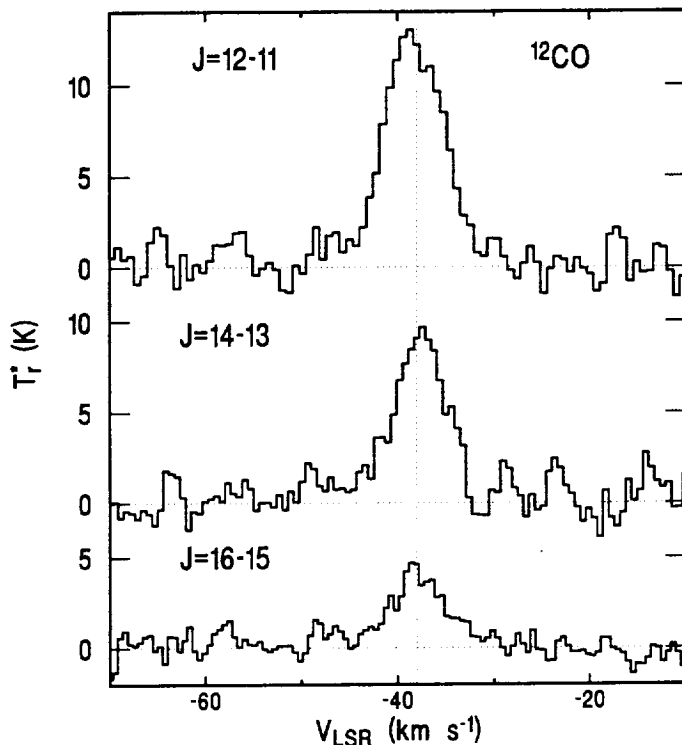
Fig. 1.— ^{12}CO J $= 12 \to 11$, J $= 14 \to 13$, and J $= 16 \to 15$ spectra obtained at W3 IRS5.

between intensities suggested to these authors that the ground state 119 μm transition was too weak for a single component model to be applicable. Various additional complexities were suggested; none of which completely solved the anomaly. In 1989 we observed the 119 μm line with our heterodyne spectrometer on the KAO (Betz & Boreiko 1989). Measurements at 0.6 km s^{-1} resolution clearly showed that the blue-side of the 119 μm emission was completely missing, and probably self-absorbed by subthermally excited OH in the expanding source. More recent heterodyne observations of the 163 μm OH line clearly show a striking dissimilarity with the 119 μm profile. Figure 2 illustrates the difference. The 163 μm profile is quite similar to those of high-J CO, and similarly extended spatially as well - up to $\pm 30''$. The 119 μm emission, on the other hand, is compact, with a source size much smaller than our 30$''$ beamsize. One straightforward conclusion from this observation is that the observed 119 μm and 163 μm lines are not emitted by the same gas.

We are currently reanalyzing all the available OH rotational data to come up with some general conclusions (Boreiko & Betz 1997). One apparent result is that the 163 μm emission is in fact an indicator for ground-state OH far removed from sources of collisional excitation. We say this because such OH can absorb 55 μm radiation emitted by dust and preferentially re-radiate at 163 μm. The process is simple and specific to the spectroscopy
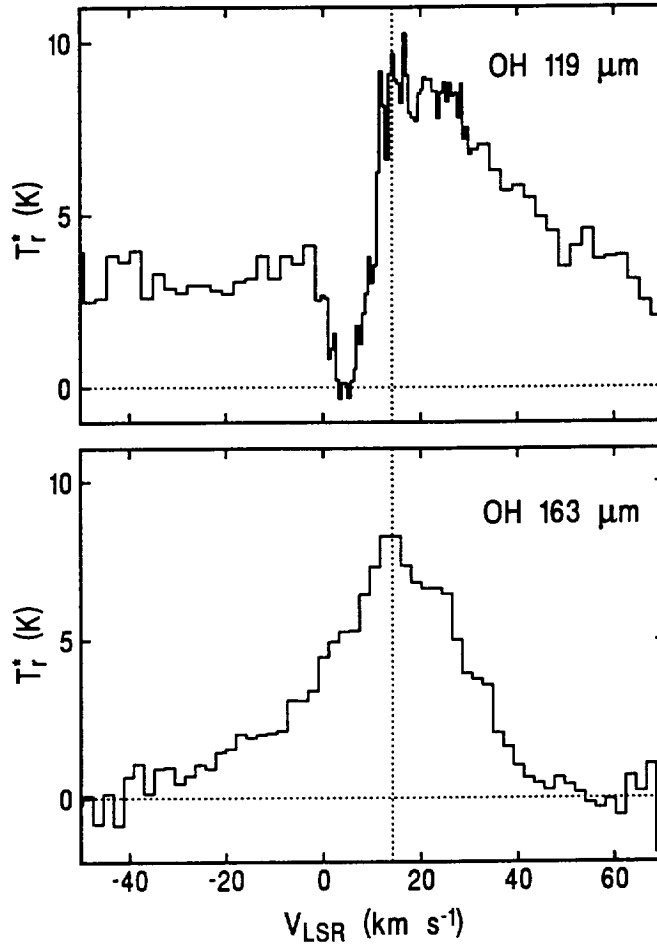
Fig. 2.— Spectra of the 119 μm and 163 μm transitions of OH from IRc2 in Orion.

of OH, but the observed intensity of 163 μm radiation is exactly what one would expect from the known intensity of dust emission at 55 μm. The linewidth of the 163 μm emission indicates the velocity dispersion of ground-state OH in the region, and is similar to that seen in high-J CO emission. The OH may be at the same temperature as the CO, but it is in the ground state because of the high critical density required for rotational excitation $(n_{H_2} > 10^{10}$ cm$^{-3})$. Once again, high resolution (plus some simple mapping) sheds new light on an old problem, in this case perhaps enough to solve it.

2.2. Selected Science Projects

Although we expect GI interest to center on high-J CO, C II , and O I observations, we have particular interests of our own that we wish to investigate, of which two examples will be given.

2.2.1. The $^{12}C/^{13}C$ Isotopic Ratio

The $^{12}C/^{13}C$ isotopic ratio of the interstellar medium is believed to be one of the most important parameters for tracing the chemical evolution of the galaxy. ^{12}C is a primary product of stellar nucleosynthesis because it can be formed in first generation, metal-poor stars, while ^{13}C is a secondary product. Thus, for successive cycles of star formation and enrichment of the interstellar medium with processed material, the $^{12}C/^{13}C$ ratio is expected to decrease with time, eventually reaching a steady-state value near 4. The solar system value of $\sim$89 is thought to be representative of the interstellar medium approximately 5 billion years ago, while the present ratio can serve as a useful check on models of galactic evolution.

The $^{12}C/^{13}C$ ratio can be measured from the relative intensities of molecular lines, such as CO, but the estimates are subject to uncertainty because of the effects of chemical fractionation, self-shielding from photodissociation, and line saturation of the more abundant isotopomer. Other observational effects, especially at millimeter wavelengths, are uncertainties in calibration because the various sets of data are not all taken with the same telescope pointing and receiver setting.

An excellent way of measuring the $^{12}C/^{13}C$ ratio, at least in photodissociation regions, is to observe the 158 μm lines of ^{12}C II and ^{13}C II . The ratio can be obtained directly from the relative intensities of the lines, as long as the stronger ^{12}C II line is not optically thick. In sources such as M42, however, the ^{12}C II optical depth is on the order of unity, and corresponding corrections must be made. The best way of estimating the ^{12}C II optical depth is to also measure the O I line at 63 μm. Emission from O I comes from the same PDR gas as that from C II (approximately), and because of the significantly higher optical depth of the O I line, it is an excellent indicator of temperature. Of course, in reality one must also consider the possibility that the O I is subthermally excited, but this problem can be handled, too. Once we know the gas kinetic temperature, we can estimate the ^{12}C II optical depth from its measured peak line intensity. Here we depend on the high resolution of heterodyne spectroscopy, because we need to know the true peak ^{12}C II intensity and the line can be as narrow as 4 km s^{-1}. We also must be able to separate the ^{12}C II emission from the 3 weaker ^{13}C II emission lines, the strongest of which is only 11 km s^{-1} away. This procedure has been used effectively for M42, where we derived a $^{12}C/^{13}C$ ratio of 58, in agreement with the value obtained from an empirical relationship between the isotopic ratio and Galactocentric distance (Boreiko & Betz 1996).

It is our goal to measure the $^{12}C/^{13}C$ ratio in a variety of clouds within our Galaxy, and to extend the technique to nearby galaxies such as the Magellanic Clouds. The small beam size of SOFIA and the high sensitivity of the HEB mixers (to be described later) are essential to this effort.

2.2.2. HeH^+ at 149 μm

HeH^+, the product of the two most abundant elements in the universe, is the simplest closed-shell heteronuclear molecule. Its existence in astrophysical environments has been a subject of interest ever since the possibility was first suggested by Dabrowski and Herzberg (1977). Later Roberge and Dalgarno (1982) extended several theoretical studies on the abundance of HeH^+ and concluded that emission in the $J = 1 \rightarrow 0$ rotational line at $149.13\,\mu m$ (2010 GHz) may be detectable from H II blisters on the peripheries of molecular clouds. Any observation of this ion that allows its abundance to be measured would be quite important for validating chemical modeling codes. HeH^+ , besides being significant in its own right, is also an important intermediary in many basic reactions of ion-molecule theories of molecular clouds. It also offers the intriguing possibility of being a direct indicator of high intensity X-ray phenomena in accretion disks and other compact occluded regions.

Emission by HeH^+ in Dense Molecular Clouds

HeH^+ is expected in dense clouds where X-ray or XUV photons are present. The ionizing radiation produces vibrationally excited H_2^+ which reacts with He atoms to form HeH^+. Collisions with H_2 are the dominant loss mechanism for HeH^+. Roberge and Dalgarno (1982) give a formula for the minimally expected flux in the $149\,\mu m$ HeH^+ line from a cloud where a stated number of H_2 molecules s^{-1} are ionized. The estimate is a lower limit because it assumes that the J=1 rotational level is only populated by the formation process. The O and OB associations which produce this ionization often appear concentrated at the edges of dense clouds, where they can burn blister-like H II regions. In such regions we might expect to see $149\,\mu m$ emission. Their line flux formula gives an estimate of $2 \times 10^{-11}\,\mathrm{ergs\,cm^{-2}\,s^{-1}}$ at $149\,\mu m$ from a source 0.5 kpc away (e.g., M42). With the SOFIA telescope this flux produces an antenna temperature T_r^* of 14 K or more at the center of a line 5 km s^{-1} wide, or half that for a 10 km s^{-1} wide line. These are strong lines that can easily be detected with our spectrometer. Despite its intrinsic uncertainties, the estimate underscores the feasibility of detecting HeH^+ in emission at $149\,\mu m$. Furthermore, the total line flux could be higher, because the calculation neglects the effects of ionization of H_2 by helium recombination photons and the excitation of HeH^+ by collisions. On the down side, although the minimum T_r^* estimate assumes that the emitting source is several times larger than the 15″ beam, it could be larger. But increased flux could be available from side-illuminated ionization fronts (blisters) seen edge-on.

Since our system noise temperature should be no worse than 2000 K (DSB) near 2010 GHz, we can detect a 0.4 K line of 5 km s^{-1} linewidth at the 5 σ level after a 20-minute integration. A 7 or 14 K line is strong enough that details in the lineshape could be explored for comparison with C II and high-J CO spectra taken at similar 0.5 km s^{-1} resolution. If the theoretical predictions hold true, in a 1-hr flight leg we could also map an extended region for comparison once again with other species found near PDR regions.

If collisions are infrequent enough to maintain much population in the J=1 level, it may prove more productive to search for the 2010 GHz line in absorption, such as against the strong continuum of IRc2 in M42 or Sgr B2. This is the approach that led to the detection of a line at the 1370 GHz frequency of H_2D^+ (Boreiko and Betz 1993). To see HeH^+ in absorption against a 4 K continuum, we will need column densities in the range of 4×10^{12} cm^{-2} to yield a 15% absorption over a 10 km s^{-1} linewidth, similar to that seen in the 1370 GHz line. The integration time required for a 5 σ detection of a 0.6 K absorption line of 10 km s^{-1} linewidth is about 30 minutes.

Emission by HeH^+ in Gaseous Nebulae

In ionized nebulae HeH^+ is produced by a number of pathways such as radiative association of He^+ with H, or H^+ with He, or by reactions of vibrationally excited H_2^+ ions with He atoms. Conversely, HeH^+ is destroyed by dissociative recombination with electrons, by photodissociation, and by reactions with either atomic or molecular hydrogen. A theoretical paper by Cecchi-Pestellini and Dalgarno (1993) discusses the comprehensive chemistry of HeH^+ in ionized nebulae in general and in the source NGC 7027 in particular. Their calculations reaffirm the estimates of Roberge and Dalgarno (1982) that HeH^+ abundances on the order of 10^{12} cm^{-2} can be expected in nebulae if the effective temperature of the ionizing source exceeds 50,000 K. The intensity of the $J = 1 \rightarrow 0$ line at 149 μm is proportional to the path integral of the electron density n_e and n_{HeH^+}, provided that n_e is not so large that the excited state is quenched (i.e., $n_e < 10^7$ cm^{-3}). For $n_e < 10^6$ cm^{-3}, the HeH^+ molecules reside mostly in the $J = 0$ level.

Cecchi-Pestellini and Dalgarno (1993) predict specific intensities for the planetary nebula NGC 7027, for which detailed models of the temperature and density structures are available. For the 149 μm line they predict a flux of $\sim 2 \times 10^{-12}$ ergs cm^{-2} s^{-1}. With the SOFIA telescope this flux produces an antenna temperature more than 1 K (depending on source size) at the center of a line 10 km s^{-1} wide, which we can detect easily on one 30 minute flight leg.

One important observational problem with detecting HeH^+ is that a strong line of atmospheric O_3 falls 260 MHz (36 km s^{-1}) below the frequency of the HeH^+ line. Consequently, observations are best done when the source has a net blue shift. Another potential problem, albeit only for lower resolution instruments, is that the HeH^+ line frequency is close to those of several strong CH lines. Although ISO may have the sensitivity to detect HeH^+ in some sources, it probably doesn't have the spectral resolution to distinguish HeH^+ from CH. This is a good problem for SOFIA.

3. Justification for Airborne Observations

3.1. Observational Requirements

The 50-200 μm interval of the far-infrared spectrum is absorbed by atmospheric water vapor which precludes groundbased observations, even from sites at the South Pole. Although theoretically a 10-15% transmission at certain far-infrared wavelengths can be obtained under ideal conditions at the South Pole, for practical astronomical purposes this transmission is not useful. Far-infrared observations must necessarily be done above the tropopause where the residual water in a vertical column is less than 15 μm precipitable. Under these conditions most of the FIR spectrum is observationally accessible, aside from the specific transition frequencies of water vapor, molecular oxygen, and ozone. The improvement in atmospheric transmission with increasing altitude is as much a function of reduced pressure broadening as reduced water abundance, because many water lines are saturated. Far-infrared absorption by high altitude ozone cannot be mitigated by observations at aircraft altitudes, but fortunately the ozone problem is not nearly so severe as that from water vapor.

3.2. SOFIA's Spectroscopic Advantage

In planning a research program for a new instrument, it is important to take into account existing observational facilities and those planned which may be competitive with SOFIA for high resolution studies of star formation.

The big advantage of SOFIA over the KAO is simply its bigger size. The 3-fold improvement in telescope aperture is particularly significant for observations of compact regions, such as the cores of molecular clouds. Observations with ground-based interferometers at millimeter wavelengths on a scale-size of a few arcsec are currently the best way to study cloud cores. The 2.5 m aperture of SOFIA will produce a diffraction limited beamsize of 8″ at λ =100 μm, which puts it on approximately equal footing (resolution wise) with mm wave interferometers and the largest ground-based submillimeter telescopes. Because SOFIA can observe in the far-infrared, however, it alone will be able to observe the dominant cooling lines of high-J CO, the most pervasive molecule other than molecular hydrogen. No other observational facility, either existing or planned, has the same combination of sensitivity, spatial and spectral resolution needed to study CO in star formation regions in such detail.

Of all the infrared facilities either in place or planned for space-based observations, only SOFIA will have the capability to do high resolution spectroscopy over the entire far-infrared spectral region from 50 to 200 μm. Conversely, because most space observatories will have excellent imaging capabilities over large fields, it is also appropriate that SOFIA emphasize high resolution spectroscopy to complement the imaging capabilities of space observatories

such as ISO, SIRTF, and FIRST. Similarly, because SOFIA has a larger aperture than ISO or SIRTF (and perhaps no smaller than FIRST), it is also appropriate that SOFIA emphasize observations requiring high spatial resolution, such as the aforementioned cloud cores and protostellar regions.

For high resolution spectroscopy SOFIA will be unmatched. ISO covers the 45-190 μm band, but only with a resolving power of 10,000 from a scanning Fabry-Perot. Its beamsize is also more than 4 times larger. IRTS has a far-infrared line mapper instrument (FILM) for the 63 μm and 158 μm channels (O I and C II, respectively), but the resolving power is only 400 and the FOV is 8×13'. SIRTF will only have a spectrophotometric capability between 50 and 100 μm, with a resolving power of 20, and is not really suited for line work in the far-infrared. SWAS will have approximately the spectral resolution of the our SOFIA spectrometer (1 km s^{-1}), but operate at longer wavelengths (538-615 μm) with lower sensitivity (T_{sys} = 4000 K SSB) and angular resolution (3.3×4.3').

Of all the pending and planned missions only FIRST offers any competition for SOFIA in high resolution spectroscopy. FIRST is planned to have a 3-m telescope (similar to SOFIA), SIS type heterodyne receivers up to 1.2 THz, and probably a Fabry-Perot spectrometer for the far-infrared. But since FIRST is scoped for launch in 2006-2010, it likely will be relegated to mop-up operations following SOFIA's discoveries of the decade prior. Of course for observations of molecules like H_2O and O_2 which cannot be done from aircraft altitudes, FIRST will have unique capabilities. But for observations of CO, HD, O I C II and many other species, SOFIA will have first crack, and so FIRST will not be *first*. SOFIA will also be able to continuously improve its focal plane technology, whereas FIRST, by nature of being a spacecraft with long leadtimes, will necessarily fly with "obsolete" focal plane instrumentation. This conclusion may appear biased, but it also may be true.

4. Instrument Concept

4.1. Overview

The current design for the heterodyne spectrometer calls for a dual band unit covering the wavelength range between 50 and 200 μm. The low band portion covers 1.5-3.0 THz (100-200 μm), and the high band spans 3-6 THz (50-100 μm). Spectral lines in each of the two bands are observed independently and simultaneously. Figure 3 shows that the input radiation is split by a high-pass beamsplitter, with the transmitted beam going to the 3-6 THz receiver and the reflected to the 1.5-3.0 THz system. The mixers for each band are contained in identical but separate dewars, with the active devices cooled to 2 K. Both the high-band and low-band mixers are Hot Electron Bolometers (HEBs) of sub-micron dimensions. FIR radiation is coupled into these devices by integrated planar antennas, of a type appropriate for each band. The tunable LO for the low band receiver is a harmonic of a frequency-tripled Gunn oscillator. The tunable LO for the high band system is a sideband

modulated FIR laser. LO coupling in each case is provided by a dielectric beamsplitter, and the combined beams are focused onto each mixer by a small silicon lens inside the dewar. Actually there are 2 HEB mixers in each dewar, and the unput radiation is separated into orthogonal polarizations and separately focused onto each mixer. This latter detail is not illustrated in the figure for simplicity. The IF output from each mixer (there are 4) is amplified over a minimum 4 GHz bandwidth and directed to an acousto-optic spectrometer (not shown) for signal processing.

There are many advantages to a dual band system. For example, one major motivation to simultaneously observe the 63 μm O I line and the 158 μm C II line. Numerous other combinations are possible, such as the 121 μm and 205 μm lines of N II, high- and low-J CO lines, and many more depending on scientific interest. Simultaneous observations make sense from a scientific point of view because identical pointing can be maintained for compared spectra. It also makes sense to make optimal use of expensive telescope time, and to provide an in-flight "back-up" capability in case of technical problems with one receiver (not that we've ever lost a flight to such in 11 years of KAO work).

It is true that the necessary integration time for dual band observations will be dictated by the weaker line. One might think that the two observations might equally well be done sequentially with a tunable receiver. This conclusion ignores the fact that the real drain of time is that of setup and preparation, and that these matters are best done on the ground before flights. Also the necessity of calibration in flight for multiwavelength observations is best done simultaneously, rather than arduously tuning and retuning the receiver (if possible) multiple times per flight. Calibration flight legs on the Moon or a planet are easy to schedule for short periods of less than 30 minutes, but must be longer if part of the calibration leg must be spent retuning the receiver. Remember that the quality of data for the entire flight depends on the quality of data from the calibration leg. Experienced observers know that the best calibrations are achieved when nothing is touched between the source and calibrator legs.

Another consideration is the required setup time for the instrument preceding flights. Far more real time is required to prepare the instrument than to actually fly it. With the dual band system these preparations can be done on the ground, where they belong, rather than in flight as would be the case for sequential observations. Furthermore, our planned dual band observations will be at wavelengths so separated that in most cases separate mixer systems (i.e., precooled dewars) will be required. Each mixer has a -3 dB bandwidth of 50%, so a single mixer could not sequentially observe the 158 μm C II line and then the 63 μm O I line. A dual band receiver with two pretuned mixers is required to observe both lines on a single flight leg. The dual band receiver provides at minimum a factor of 2 savings for flight time compared to a single band unit, and overall less work for the observing team when the science demands that both lines be observed.

As stated above, we have also designed the receiver to separate and detect orthogonal polarizations. This will give us a $\sqrt{2}$ improvement in S/N ratio for extra high sensitivity

observations. A better way to look at this is that the spectrometer takes data twice as fast, and one flight with dual polarization detection is worth 2 flights without. This is best done by combining LO and signal beams with a 90/10 dielectric beamsplitter and focusing the beam into the dewar where a wire grid beamsplitter (at 45 degrees to the LO's linear polarization) separates the two linear polarizations. The transmitted and reflected polarizations are then focused onto separate HEB mixers.

The basic design of the spectrometer is similar to that of our now retired KAO receiver. Key improvements of the SOFIA instrument over the KAO system are a switch to superconducting and quantum-noise-limited detectors (mixers), tunable local oscillators as required, and the dual wavelength and dual polarization capabilities mentioned above. Furthermore, a limited capability for multibeam observations (array detectors) could be provided, but not implemented until after the first year or two of operations. This would require eliminating dual polarization detection, however. Each receiver could have 6-8 mixer elements in a linear or close-pack array if there is sufficient scientific demand for mapping. Large focal plane arrays will not likely be required; besides, they are cumbersome because each element requires a separate IF signal processor. Mapping at low spectral resolution is probably better done with other instrumentation, particularly that designed for space-based observatories.

Only recently has far-infrared mixer technology advanced to the point where a spectrometer such as this could be taken seriously. Critical breakthroughs in HEB mixer technology have occurred in the past three years that allow a more sensitive, compact, and versatile spectrometer to be designed. From our experience on the KAO, we understand that ease of use is also an important design factor. Although the new spectrometer is more complex than the KAO instrument, with proper design we can simplify and automate operational procedures so that it is more "user friendly" for Guest Investigators.

4.2. Spectral Resolution

The spectral resolution of the receiver is dictated by the channel widths of the analyzer which processes the IF signals from the mixer. The ultimate resolution is limited by the stability of the local oscillator and can be as narrow as 30 kHz for a heterodyne spectrometer. In practice, however, it is generally not productive to use a resolution significantly finer than the widths of the expected spectral features. There are exceptions of course, for example when minute details of the line profile are being scrutinized in a high signal-to-noise situation. Generally we find that a resolution of 0.3 km s^{-1} is adequate for astronomy. This translates to a channel width of 3 MHz at 3 THz. One advantage of the heterodyne spectrometer over a scanning instrument is that many spectral channels can be analyzed simultaneously. On the KAO we used a single acousto-optic-spectrometer (AOS) as an analyzer with 1000 channel capacity. For the multiple mixers on SOFIA we intend to use 3 AOS signal processors with a total of 3000 channels spanning a total of 5.2 GHz. For

the non radio astronomers, one should view this multichannel capacity analogously to using an echelle grating with a large array detector.

4.3. Estimated System Performance

Rather than attempt incremental improvements in the sensitivity of the Schottky mixer technology we used on the KAO, we have instead decided to abandon it altogether. Our new look for the next millennium will feature a superconducting mixer technology that should approach quantum limited sensitivities during the SOFIA era. The mixers will be Hot Electron Bolometers (HEBs), which have been shown in the lab to have the best noise performance at far-infrared wavelengths, and which also show the best promise for significant improvements in sensitivity.

For heterodyne receivers the usual expression of sensitivity is the Rayleigh-Jeans equivalent system noise temperature, T_{sys} (SSB), which is independent of bandwidth. The RMS noise level ΔT in a bandwidth B after an integration time t can be computed from T_{sys} as:

$$\Delta T = \frac{1}{\eta_c} \frac{2T_{sys}}{(B \cdot t)^{1/2}} , \qquad (1)$$

where the factor of 2 arises from the 50% duty cycle of beamswitching. Here $\eta_c = 0.6$ is the net coupling efficiency between the receiver and the telescope (see next subsection). The noise-equivalent-power (NEP) of the receiver on the telescope can then be readily calculated from ΔT in a 1-second integration:

$$NEP = 2k\Delta T \cdot B = \frac{1}{\eta_c} 4kT_{sys}B^{1/2} \ (\mathrm{W\,Hz}^{-1/2}) . \qquad (2)$$

An additional factor of 2 loss has been included in the NEP to account for the fact that we detect only one of two available polarizations. This loss is real only for unpolarized sources when we want to compare NEP's with an incoherent type detector. Here rather than NEFD we quote NEP because it is a more relevant indicator of sensitivity for an instrument designed to detect narrow spectral lines. From the equation above, we see that an arbitrarily low (but valid) NEP can be quoted simply by assuming an arbitrarily narrow bandwidth B. For practical observations, however, the resolution need not be much narrower than 10% of the linewidth.

For comparison purposes we can calculate our NEP at 158 μm (the wavelength C II fine structure line). At 158 μm (1.9 THz) our system noise temperature will be less than 2000 K (DSB), equivalent to 4000 K (SSB) (Skalare et al. 1997; Karasik et al. 1997a). The corresponding NEP for a bandwidth of 31 MHz equal to a typical linewidth of 5 km s^{-1} is 2.0×10^{-15} W Hz$^{-1/2}$. Within this interval, however, there are ~10 3.2-MHz resolution elements, and thus on a per-channel basis an NEP 3 times lower could be quoted.

Our heterodyne receiver is as sensitive as a Fabry-Perot spectrometer with an NEP of 6.9×10^{-16} W Hz$^{-1/2}$ and a true resolution of 5 km s^{-1} that would need to be scanned over the 166 km s^{-1} bandwidth of our 1 GHz AOS. The comparison includes the fact that the Fabry-Perot detects both polarizations. The heterodyne receiver's chief advantage is that at wavelengths $>100\,\mu$m this sensitivity has been achieved simultaneously with a spectral resolution (and velocity-scale accuracy) more than an order of magnitude higher than any other FIR spectrometer. Of course, if the emission lines are wide, then the superior resolution of the heterodyne spectrometer is less important, unless it is necessary to avoid interfering atmospheric lines.

Another significant difference between a heterodyne spectrometer and a Fabry-Perot is the difference in the line shape function. For instruments with similarly quoted resolution (FWHM) the line shape of the spectral channel of the heterodyne spectrometer is usually Gaussian, whereas that of the Fabry-Perot is Lorentzian. What this means in practice is that the heterodyne instrument is far better in distinguishing a weak line from interference by a nearby strong line. As the sensitivity of all types of instruments increase, the limiting sensitivity for line detection will be governed more by confusion from nearby lines rather than raw instrumental sensitivity. Such is currently the case in millimeter and submillimeter line spectroscopy (Sutton et al. 1985; Schilke et al. 1997), and the same may hold true at least up to 3 THz, where hν is still on the order of kT. Here T is the kinetic temperature of the molecular cloud. So true resolution, governed by the equivalent width of the instrumental line function, may soon be just as important as NEP for the detection of weak FIR lines. One final point is that the frequency calibration of the FIR heterodyne spectrometer is usually good to 1 part in 10^7, which is similar to that of a good mm-wave spectrometer.

4.4. Coupling Efficiency

The HEB mixers described above are coupled optically to the telescope with off-axis mirrors. Mode matching is done so that the more or less Gaussian main beam response of the mixer fills the primary aperture with a -8 to -12 dB tapering of response toward the edge of the primary mirror. With such coupling the beam pattern on the sky is also approximately Gaussian with a FWHM beamwidth given by λ/D. The beam pattern from a single mixer is matched to the central diffraction lobe of the telescope. One can in principle provide for a multi-beam response with multiple mixers in the focal plane, as was mentioned earlier.

The fraction of incident flux from the telescope that is coupled into the receiver is a measure of the aperture efficiency. For a receiver which has an approximately Gaussian beam pattern for the accepted spatial mode, the aperture efficiency can be readily calculated as a function of the secondary mirror blockage ratio. For a ratio of 0.2 as applies to the KAO or SOFIA, the best coupling efficiency is about 0.74 for an edge taper of -10 dB.

Taper refers to the relative amplitude of the receiver's Gaussian beam at the edge of the secondary mirror. Underilluminating the telescope (a higher f/#) causes more power to be lost by the central blockage, whereas overilluminating (a lower f/#) causes power to be lost over the mirror peripheries. The optimum edge taper lies between -8 and -13 dB, and will give the above efficiency within a few percent. A telescope built without a central blockage can yield an aperture efficiency as high as 0.82, so the loss from the central blockage is not serious, although it is higher than what would be calculated from the secondary to primary mirror area ratio. Most antenna coupled mixers used in submillimeter and far-infrared heterodyne receivers have approximately Gaussian beam sensitivity patterns and the above calculation is valid.

We estimate an aperture efficiency of 0.7 for the antenna coupled HEB mixer on SOFIA. This estimate is based on our 11 year experience with Schottky mixers on the KAO, where we measure aperture efficiencies within a few percent of the theoretical maximum. (It's not hard to do when all mirror surfaces have been figured to optical tolerances.) Also of concern are the reflection losses of the 3-mirror telescope system. Our measurements at FIR wavelengths on the KAO show that reflectivities >95% are easily obtained even on old surfaces. Nevertheless this reflection loss reduces signal levels by ≤14%. The overall coupling efficiency is thus about 0.6 . This is the value used for the NEP calculation in the previous subsection.

Another potential term in the coupling efficiency is the transmission of the aircraft pressure window (if it exists). On the KAO we used a 3 in. dia. x-cut crystal quartz pressure window. The surfaces were AR coated with polyethylene and losses were low up to 2 THz. Beam paths in the spectrometer were open to the cabin environment. On SOFIA we intend to work at higher frequencies, where losses from a 0.25" thick pressure window (and from the air in the cabin environment) become intolerable. Consequently, the beam path will be fully enclosed so we can run "open port" and have no window losses.

4.5. Low Band Receiver: 1.5-3.0 THz (100-200 μm)

Hot-Electron Bolometer Mixer

For observations in the 100-200 μm range we intend to exploit the advantages of the new hot electron bolometer (HEB) mixers. These devices have been developed over the last couple of years by McGrath, LeDuc, and co-workers at the Center for Space Microelectronics Technology at the Jet Propulsion Laboratory in collaboration with the research group of D. Prober at Yale. The basic design and expected performance of the HEB mixer has been described by Prober (1993). The superconducting element is a Nb film of submicron dimensions that bridges the gap between two normal-metal wire leads. Theoretically, the thermal response time of such a device can be extremely fast (<20 ps), which would enable IF response as high as 9 GHz for 0.08 μm long devices (Burke et al.

1996; Bumble & LeDuc 1997). The device is cooled to about 2K, a temperature below the reduced superconducting transition temperature of 5-6 K for ultrathin ($\sim$100 Å) Nb films. The combined DC, local oscillator, and signal fields heat the electrons in the thin film above the lattice temperature. The device resistance is a function of the electron temperature, which is modulated at the IF. Thus an IF output response is obtained from the DC bias. The sensitivity of one of the first Nb microbolometer mixers was 650 K (DSB) at 533 GHz (1300 K SSB), which is within a factor of 2 of the best sensitivity achieved with Nb SIS devices in the same receiver at this frequency (Skalare et al. 1995; Skalare et al. 1996). The IF signal bandwidth was about 2 GHz, which is consistent with the 0.3 micron length of the Nb microbridge. The measurements were done with the HEB device in a waveguide mixer mount.

Microbolometers can also be readily integrated with planar antennas such as spirals, slots, and twin dipoles to achieve optimum matching between the radiation field and the active device. Planar antennas are more appropriate than waveguide at far-infrared wavelengths. In the configuration selected here, radiation is coupled into the HEB element by a twin slot antenna on a planar substate. The free space antenna response is modified by an elliptical silicon lens bonded onto the substate. The resulting beam is concentrated in the forward direction, and can be readily matched to the telescope. The general design of the mount is similar to that described by Bin et al. (1996) for lower frequency SIS mixers.

At 2.5 THz the best result with an optically coupled HEB mixer is a receiver noise temperature of 3000 K (DSB) (Karasik et al. 1997a). The -3 dB input bandwidth of this mixer extends from 1.5 to 2.5 THz, so the heterodyne measurements would undoubtedly have been better if measured at 2.0 THz. With a modest correction for the antenna roll-off at the measured frequency of 2.5 THz, we estimate that a receiver noise temperature of 2000 K (DSB) would have been measured at 2.0 THz. Regardless, at 2.5 THz the current HEB performance corresponds to a mixer quantum efficiency η better than 3% at 2500 GHz, about a factor of 4 better than the best achieved with a GaAs Schottky mixer at this frequency (Betz & Boreiko 1993). A major goal before SOFIA flies will be to achieve another factor of 2-3 improvement over this conservative estimate to get a net $\eta = 0.1$. Much of this gain can be achieved by more efficient coupling of radiation into the device (e.g., AR coating the Si lens, lower filter losses, peaking the antenna response for the frequency of interest).

HEB devices with active lengths of 0.15 μm indicate IF noise bandwidths of about 3-4 GHz. More generally, measurements on HEB devices by Burke et al (1996) show that the IF bandwidth scales proportional to L^{-2}, when L the device length is less than 1 μm. This is intuitively the case because the thermal conductance is determined by electron outdiffusion from the ends of the microbridge. Microwave measurements by Prober's group at Yale on HEB devices fabricated at JPL with a 0.08 μm length indicate an IF signal bandwidth of at least 6 GHz. Additional measurements suggest that the IF noise bandwidth may be as high as 9 GHz. Although these improvements are slightly less than that predicted by the scaling

law, they are nevertheless quite encouraging. Currently the 0.08 μm HEBs are difficult to manufacture with the photolithographic process used at JPL, and yields are low. The larger 0.15 μm devices with 4 GHz IF bandwidths show good yields per wafer, however. Obviously, more work on the small device process is needed to improve yields.

A big advantage of the HEB mixer is that its response is thermal and essentially independent of input frequency, unlike the SIS device whose sensitivity degrades just below the superconducting gap frequency (e.g., 750 GHz for Nb). Theoretically the sensitivity measured at 533 GHz should be possible throughout the 1.5-3.0 THz (150-300 μm) region, and higher. Aside from second order considerations related mostly to antenna coupling inefficiencies, we expect to approach quantum noise limited operation as we go higher in frequency. Although SIS devices made from low temperature superconductors will likely be better than HEB mixers at frequencies below the energy gap of the material, HEB mixers will be superior at higher frequencies. HEB mixers should work well throughout the far-infrared, subject only to coupling inefficiencies from their integrated planar antennas and the unavoidable limit of quantum noise.

For the low band receiver we will mount two mixers and their associated IF amplifiers in a single LHe dewar of roughly 6 liter capacity. No other components of the receiver require cooling to cryogenic temperatures, and so the consumption of LHe will be relatively low. A 6 liter LHe dewar with LN_2 jacket should last at least 12 hours under the anticipated heat load and pumping conditions, so no in-flight refills will be required. We will perform adequate tests in the lab to ensure that the dewar capacity is correct.

An important advantage of the HEB mixer is its extremely low local oscillator power requirement (<100 nW absorbed in the Nb element). Given the current ~6 dB of mixer circuit losses and allowing for coupling losses of 10 dB from a dielectric beamsplitter, only 5-10 μW of LO power are needed. One can now use a number of tunable LO schemes that would be impossible to consider with a Schottky mixer requiring a 1 mW LO. Of course a low LO drive requirement can also be interpreted as a low saturation level for the device, and that is certainly true. For mixers using planar antennas, especially, filters will be needed to restrict the background flux on the mixer. SIS mixers at lower frequencies have similar saturation limitations, but are nevertheless quite sensitive with simple filtering of the input radiation. As a worst case example for an HEB mixer, radiation from a 300 K background within a 1 THz bandwidth centered at 2 THz will couple 2 nW of unwanted power onto the mixer element. Here a coupling efficiency of 50% is assumed. We propose to use resonant mesh filters of the type investigated by Porterfield et al. (1994) within the dewar to restrict the input radiation to a 10%-20% bandwidth centered on the desired spectral line. A small turret of such filters will necessarily be required to permit successive observations over a wider frequency range. The cooled mesh filter also helps to reject the unwanted harmonics from the low band LO, but that is a discussion for the next section.

Blocked-Impurity-Band Photoconductive Mixers

As part of this effort we investigated BIB devices as far-infrared photomixers. This was intended to be an alternative mixer technology to the HEB devices mentioned earlier. Ga:Ge BIB photoconductors developed at Rockwell Science Center (now a part of Boeing) for the SIRTF program were acquired from Prof. D. Watson at Univ. Rochester and were evaluated as high speed mixers. Unfortunately, our test results on these particular BIBs were not successful. The problem arise from fabrication anomalies of the particular devices tested, rather than the intrinsic capabilities of the device. The tested devices had been fabricated with an undesirable spike in donor impurities in the active region underneath the blocking layer. As a result, the depletion depth under nominal bias conditions was minimal. Consequently, the response time was slow and the devices easily saturated when the necessary amounts of local oscillator power were applied. These devices represented an early attempt at epitaxial growth of the material, and this particular problem can be easily eliminated in subsequent fabrication runs. However, now that the SIRTF program has chosen traditional (non-BIB) Ga:Ge photoconductors for its far-infrared detectors, further work at Rockwell on Ga:Ge BIB detectors is not planned, at least for the foreseeable future. No other source exists for these devices, so we come to a dead-end - for now.

Toward the end of the project we obtained samples of As:Si BIB detectors from the Rockwell science Center (now part of Boeing). These devices work in the 15-30 micron spectral region and can be fully depleted under nominal bias conditions. Consequently they should have the fast response times we need for mixer applications. Sufficient time was not available to test the Si-BIBs, however, and the work must be deferred to some subsequent grant.

Local Oscillator: Harmonic Multiplier

We intend to use harmonic generators with a microwave source to synthesize a tunable LO signal for the 1.5-3.0 THz band. An unoptimized harmonic generator using a frequency tripler and a cascaded tripler-quintupler (n=3,4,5) with a variant of a corner cube reflector should work (see Figure 3). The goal for the generator will be 0.1% efficiency for generating (overall) the 9th, 12th, and 15th harmonics from a 40 mW TED (Gunn) oscillator running at 125-140 GHz. The TED oscillator and waveguide frequency tripler are commercially available. Output from the waveguide tripler should be about 4 mW in the 420 GHz frequency range. We would like 500 nW of LO power on the HEB mixer at 2 THz. Allowing for a 10% beamsplitter we would therefore need 5 μW from the tripler-quintupler, which is driven by the 4 mW signal at 420 GHz. Zimmermann and co-workers (1995) have already produced 60 μW at 1 THz, and 20 μW at 1.46 THz (Zimmerman 1997) with resonant multipliers. We view our LO requirements as modest and quite achievable. Although we have restricted the application of harmonic generation to LO frequencies <3 THz, the range may in fact be higher, and the technique may also be useful for part of the frequency range of the high band receiver (3.0-6.0 GHz). Our particular harmonic generator design is based on the corner reflector mixer design we have used successfully with Schottky diodes for over 12 years. The multiplier is inherently broadband because there is only 1 resonant element

(the reflector spacing). For the same reason the efficiency is low, but then so is the required output.

Our plans for dual polarization detection mean that there will be 2 mixers and therefore we will need twice the LO power stated above. Should the harmonic generator not be up to the task, we need to plan for an alternate low-band LO. There are two backup designs. One is to use a commercially available harmonic generator of the type made by Zimmerman (1997), but there would undoubtedly be engineering costs associated with extending performance to 2 THz and above. A more economical backup solution is a sideband generator with a far-infrared laser (identical to that proposed for the high band LO). This technique works well, but would increase the size of the instrument because a second laser would be required. It is not otherwise a big problem. We should have enough data on multipliers to make an LO decision before the end of the year, and in time for the preliminary program review of the basic instrument design.

Currently, the design volume of the low band receiver is about 0.5 x 0.5 x 0.5 m^3, and the mass is 30 kg (66 lbs.).

4.6. High Band Receiver: 3.0-6.0 THz (50-100 μm)

HEB Mixer

HEB mixers for the 3.0-6.0 THz band have yet to be fabricated, but some thought has been given to optimum geometries and antenna structures. For example, the smaller antenna dimensions may dictate a change from twin-slots to a spiral design. At higher frequencies a wider IF bandwidth would also be desirable, but not absolutely required. The 0.15 μm Nb devices with a 4 GHz IF would should work well with a tunable LO. On the other hand, the wider IF bandwidth available from the 0.08 μm Nb devices would allow us to use a fixed-frequency laser LO in many cases.

As stated before, A big advantage of the HEB mixer is that its response is thermal and essentially independent of input frequency (Karasik et al. 1997b). Hence we may with confidence make some extrapolations on high band mixer performance, even though measurements between 3-6 THz have yet to be made. A conservative approximation would be to assume a coupling efficiency between the planar antenna and the mixer proportional to ν^{-2} (e.g., efficiency at 5 THz would be 25% of that achieved at 2.5 THz). This would lead to an expected noise temperature of 12,000 K (DSB) at 4.75 THz (the 63 μm O I line), based on 3,000 K (DSB) performance at 2.5 THz, which has been measured. Of course we hope for better numbers by the debut of SOFIA in 2001. This high frequency goal is 4 times worse than the noise temperature at 2.5 THz, but nevertheless 7 times better than the GaAs Schottky mixer we used to make the first heterodyne observations of O I in 1995 (Boreiko and Betz 1996a). We should repeat that this is a goal, and no guarantees can be given that unknown problems will not prevent its attainment. Nevertheless, the goal seems

realistic, given our current understanding of HEB physics.

Work on the 3-6 THz mixers will begin with a study of planar antenna structures such as spirals which appear to offer advantages over slot antennas when circuit dimensions get small. Although prototype high band mixers could be fabricated under this proposal, a dedicated engineering effort to optimize high band mixers will not be possible with the current budget. Undoubtedly supplemental funding will be required from the SOFIA detector development program. Support for the development of 3-6 THz mixers with IF bandwidths exceeding 6 GHz will likely produce better devices, appropriate for SOFIA. The cost of detector development must be weighed against the cost (and availability) of flight time. A factor of 2 to 4 improvement in mixer sensitivity will speed attainment of science goals by a factor of 4 to 16, and enable some projects which otherwise would be impossible given the limited flight time for the Observatory.

Local Oscillator: Laser with Sideband Generator

Although fixed-frequency far-infrared gas lasers are eminently practical as local oscillators with wide-band Schottky diode mixers, they do not offer same utility for mixers with more limited IF bandwidths. The FIR lines of many important species like CO, C II , and O I can still be observed, but complete coverage of the FIR spectrum is no longer possible. The spectral density of available FIR laser lines is just not high enough for a mixer with a limited 4 GHz IF bandwidth. Should IF bandwidths of newer HEB mixers reach 9 GHz, then the last statement is not quite so true. Regardless, the LO power requirement for an HEB mixer is low enough that and we can use frequency modulation techniques to produce tunable sidebands around the carrier frequency of a fixed frequency laser line. Spectral filtering and phase cancellation techniques (a diplexer) can then be used to select the desired LO sideband and reject the image sideband and carrier frequency radiation. The technique has been used successfully for many years as a tunable source of FIR radiation at a power level of a few μW for laboratory spectroscopy (Farhoomand et al 1985; Blake et al 1991). With the newest GaAs mixing diodes, the tunable output should be more than adequate to drive HEB mixers. Note that with ± 140 GHz tunable sidebands on a CW laser carrier, there is no need to list frequency coincidences with target lines, because we have almost complete FIR frequency coverage. Once we get into small arrays of 6-8 elements, however, the increased LO power requirement requires us to use a fixed frequency laser LO. The wider IF bandwidth of the 0.08 μm HEB device will then be essential to achieve frequency coincidence between a laser and a target line.

We are aware of the many interesting technologies that may provide alternative LO solutions at FIR wavelengths. Near-IR diode lasers and photomixers, difference frequency generation in the nonlinear crystal GaP, difference frequency generation between CO_2 lasers using multiple quantum well mixers, Russian BWOs, are all examples of new LO technologies currently being investigated in other laboratories. None of these variants offers any improvement in power, stability, or accuracy over the FIR laser system we have selected. Although the alternatives have particular advantages over a FIR laser in one

aspect or another, they are all in the early stage of development and too immature to propose for SOFIA at this time. For example, we investigated far-infrared signal generation from difference frequency generation between two different ^{12}CO laser lines. A beat signal in the THz range can be generated by focusing the ^{12}CO beams onto an antenna coupled to a metal-insulator-metal (MIM) point contact diode. We investigated Ni-W, Ni-CO, and Ni-SnTe point contacts. Although both second- and third-order mixing products were generated, the MIM diodes were mechanically unstable, despite efforts to improve robustness. Although vacuum-deposited planar versions ' of these diodes should solve the stability problem, there remains the excess shunt capacitance of the planar structure. Given the limited resources and time available, we rejected this technology for the SOFIA receiver in favor of the adopted approach.

The volume and mass of the high band receiver is dictated by the size of the FIR laser and the LHe dewar. We estimate the volume to be 0.5 x 0.5 x 1.2 m^3 and the mass about 140 kg (308 lbs.). The weight estimate for the total instrument including low band receiver is thus 375 lbs. The weight could be reduced by possibly 25 % by structural analysis and removal of unnecessary material, but then more dead weights would be needed to balance the telescope.

4.7.   AOS Signal Processors

We have a 1000 channel AOS spanning 1.2 GHz bandwidth and a 1000 channel AOS spanning 2.0 GHz. These processors will require only minor enhancements for SOFIA, mostly in the area of sensor replacement (CCD replaces Reticon), and laser replacement (diode laser replaces HeNe). Other enhancements include additional computer-controlled diagnostics and calibration capabilities. As part of this work, we did complete a new control program for our existing AOS systems that uses a GUI interfaces and works unders Windows O/S. The real-time control is programmed with Testpoint software (similar to but better than LabView). Our previous software was written for DOS O/S, which is now considered obsolete.

We would like to construct a second 2 GHz AOS to get 4 GHz total bandwidth for the high-band receiver, and to use the existing 1.2 GHz unit for the low-band work. This would give us a total of 5.2GHz AOS bandwidth summed over 3 units. Other permutations of analyzers and receivers will be possible under software control. For example, the 4 HEB outputs could be multiplexed into 2 2-GHz AOS systems. We are not requesting funds for the second 2-GHz AOS in this proposal. The main cost is the Bragg cell, and we are currently looking into a surplus acquisition at considerable savings. We are not considering any larger effort in AOS construction to support future ventures into small array mixers, but will await the SOFIA program office decision on possible facility back-end systems.

Regarding the use of AOS spectrometers in the high vibration environment of an aircraft, we find no difference in performance for our systems in the air versus on the ground. Line observations on the KAO indicate that the statistical noise in the AOS spectrum after a 1-hr integration is consistent with our measured T_{sys}. We find that ΔT improves as it should proportional to $\sqrt{t}$, and we are not generally bothered by systematic sources of noise such as baseline wiggles from standing waves. Such systematic problems, were they to exist, would make quotes of T_{sys} rather meaningless as far as getting results is concerned.

Say here we have reprogrammed AOS with GUI interface.

5. Data Control and Analysis

The programming environment for instrument control will likely be a high level language called Testpoint from Capitol Equipment Co. This language permits high level programming for GPIB and RS/232 interfacing with hardware. In addition, it provides links to C, C++. -OLE, and assembly code for versatile and efficient data gathering. All electronics such as oscillators, the lock-in, synthesizer, the AOS, stepper controller, and spectrum analyzer will be interfaced via GPIB. This standard, although somewhat old and perhaps obsolete, is nevertheless cheap and quite adequate for the task at hand. The control computer for the spectrometer will link to observatory workstations over the onboard LAN, so that a workstation can function as a backup control computer.

Data analysis will be done with the IDL language, which is one of many standards in astronomy. Data files will be stored in a standardized format such as FITS, but probably only a subset of the entire specification. The guiding philosophy for software will be adoption of standard commercial components with good documentation so that the GI community can work as independently as possible.

6. Operational Issues

6.1. Instrument Reliability

The need for reliable instruments is obviously important, given the cost and complexity of flight operations. The question is how to assess reliability. We choose to answer by comparing our SOFIA instrument with our KAO experience.

The SOFIA spectrometer will use mixers, local oscillators, and control electronics which are similar to those employed on the KAO. On SOFIA, however, the mixers will be planar integrated devices capable of withstanding large mechanical shocks. The KAO

mixers were GaAs diodes which were contacted by free-standing whisker antennas. As such they were extremely sensitive to mechanical and electric transients. We expect the integrated SOFIA mixers to be far more robust in that respect. Both systems employ laser local oscillators, so there will be no change there. Both LO systems use high voltage laser power supplies and water cooling, too, so no change there. Although we cannot guarantee performance, we feel confident that the reliability of the SOFIA spectrometer will be no worse than the earlier version used on the KAO. The KAO spectrometer had 1 mixer and 1 local oscillator, whereas the SOFIA system will have 4 mixers and 2 local oscillators. So even though there is more to break on SOFIA, there is also a backup built right into the design of the spectrometer.

So what was the KAO experience ? In 11 years of flights between 1985 and 1995, we experienced 3 in-flight mixer failures. Two of these were likely caused by electrical transients (problems with A/C power system), and one failure was caused by mechanical shock. In no incident was there sufficient loss of observing time that any science objective was compromised. The average time loss was 1/2 hour per incident.

As far as the laser LO system is concerned, there were no in-flight failures in 11 years of observations. It will be hard to top that on SOFIA, so we will just hope for equivalent performance.

Computers and electronics were also fairly reliable. We had a few drop outs of the computer for periods of 15 min during the first few years on the KAO, but these problems ceased when we upgraded from an LSI-11 to a PC-AT. No other significant instrumental problems occurred, and no flights were ever lost to instrument related problems.

6.2. Co-mounted Instruments

We are considering a modification in the design of our spectrometer and its mount so that a small facility instrument, such as the IR-camera, could be co-mounted on the telescope. A flip-mirror near the gate valve entrance would divert the beam perpendicularly to the IR camera. Implementation of this capability requires coordination and agreement with the facility scientists. The rationale for dual instrument operation is that on long 9-hr flights it will be difficult to optimize the flight plan for one type of program. For example, we like to observe in the galactic plane on west bound flights. Extragalactic observers might prefer the east-bound legs. Other operational concerns such as the availability of personnel may preclude dual operations, so further study is obviously needed.

REFERENCES

Betz, A.L., and Boreiko, R.T. 1993, Astronomical Infrared Spectroscopy, ed. S. Kwok, ASP Conf. Series Vol. 41, (ASP: San Francisco 1993), pp. 349-346

Bin. M., Gaidis, M.C., Zmuidzinas, J., Phillips, T.G., and LeDuc, H.G. 1996, Appl. Phys. Lett., vol. 68, pp 1714-1716 (March 1996).

Blake, G.A., Laughlin, K.B., Cohen, R.C., Busarow, K.L., Gwo, D.-H., Schmuttenmaer, C.A., Steyert, D.W., and Saykally, R.J. 1991, Rev. Sci. Instrum, 62 (7), 1701-1716

Boreiko, R.T., and Betz, A.L. 1993, ApJ Lett., 405, L39

Boreiko, R.T., and Betz, A.L. 1995, in *Airborne Astronomy Symposium on the Galactic Ecosystem*, ASP Conf. Series, Vol. 73, (Haas, Davidson,& Erickson, eds.), 587-588

Boreiko, R.T., and Betz, A.L. 1996, ApJ, 467, L113-L116

Boreiko, R.T., and Betz, A.L. 1997 (in preparation)

Bumble, B, and LeDuc, H.G. 1997, IEEE Trans. Appl. Superconductivity, 7(2), 3560-3563 (1997).

Burke, P.J., Schoelkopf, R.J., Prober, D.E., Skalare, A., McGrath, W.M., Bumble, B., and LeDuc, H.G. 1996, Appl. Phys. Lett., 68(23), 3344

Cecchi-Pestellini, C., and Dalgarno, A. 1993, ApJ, 413, 611-618

Dabrowski, I., and Herzberg, G. 1977, Trans. NY Acad. Sci., 38, 14-25

Draine, B.T., Roberge, W.G., and Dalgarno, A. 1983, ApJ, 264, 485

Farhoomand, J., Blake, G.A., Frerking, M.A., and Pickett, H.M. 1985, J. Appl. Phys., 57, 1763-1766

Jaffe, D.T., Harris, A.I., and Genzel, R. 1987, ApJ, 316, 231

Karasik, B.S., Gaidis, M.C., McGrath, W.R., Bumble, B., and LeDuc, H.G. 1997a, IEEE Trans. Appl. Superconductivity, 7(2), 3580-3583

Karasik, B.S., Gaidis, M.C., McGrath, W.R., Bumble, B., and LeDuc, H.G. 1997b, Appl. Phys. Lett. (accepted for publication)

Melnick, G.J., Stacey, G.J., Genzel, R., Lugten, J.B., and Poglitsch, A. 1990, ApJ, 348, 161

Porterfield, D.W. et al. 1994, Appl. Optics, 33, 6046 (1994).

Prober, D. E. 1993, Appl. Phys. Lett., 62 (17), 2119-2121

Roberge, W., and Dalgarno, A. 1982, ApJ, 255, 489-496

Schilke, P., Groesbeck, T.D., Blake, G.A., and Phillips, T.G. 1997, ApJ Supp., 108, 301-337

Skalare, A., McGrath, W. R., Bumble, B., LeDuc, H. G., Burke, P. J., Verheijen, A. A., and Prober, D. E. 1995, IEEE Trans. Appl. Superconductivity, 5(2), 2236-2239

Skalare, A., McGrath, W. R., Bumble, B., LeDuc, H. G., Burke, P. J., Verheijen, A. A., Schoelkopf, R.J., and Prober, D. E. 1996, Applied Phys. Lett. (March, 1996).

Skalare, A., McGrath, W.R., Bumble, B., and LeDuc, H.G. 1997, IEEE Trans. Appl. Superconductivity, 7(2), 3568-3571

Stutzki, J. Stacey, G.J., Genzel, R., Harris, A.I., Jaffe, D.T., and Lugten, J.B. 1988, ApJ, 332, 379

Sutton, E.C., Blake, G.A., Masson, C.R., and Phillips, T.G. 1985, ApJS, 58(3), 341-378

Zimmermann, R., Rose, T., Crowe, T.W., and Grein, T.W. 1995, Proc. 6th Terahertz Technology Conf., Pasadena, CA, 21-23 March, 1995, pp. 13-27

Zimmermann, R. 1997, RPG Radiometer-physics, Bergerwiesenstr. 15, 53340 Meckenheim, Germany (private communication)